Recent freshening in the Kara Sea (Siberia) recorded by stable isotopes in Arctic bivalve shells

Johannes Simstich,[1,2] Ingo Harms,[3] Michael J. Karcher,[4,5] Helmut Erlenkeuser,[6] Vladimir Stanovoy,[7] Lyudmila Kodina,[8] Dorothea Bauch,[9] and Robert F. Spielhagen[9,10]

Received 20 September 2004; revised 17 February 2005; accepted 4 May 2005; published 13 August 2005.

[1] Oxygen and stable carbon isotope records along the growth direction on shells of the bivalve species *Astarte borealis* and *Serripes groenlandicus* reliably record all important aspects of the bottom water hydrography in the shallow southeastern Kara Sea, despite uncertainties about the isotopic range due to sparse sampling and the possibility of growth rate changes. Changing freshwater supply from the rivers Ob and Yenisei is the main cause for seasonal temperature and salinity variations near the three sampling locations in 20 to 70 m water depth as suggested by CTD measurements and modeling. Peak winter salinity of the simulated hydrographic data series and peak winter values in the isotope records follow negative trends, which indicate a freshening of the bottom water due to an increasing fraction of river water during the 1990s. This freshening affected the whole Kara Sea, and coincided with a lowering of regional air pressure gradients, as indicated by the declining Arctic oscillation index. The resulting weakening of the prevailing southwesterly winds diminished the inflow of saline Atlantic-derived water from the Barents Sea through the Kara Strait in the southwest, and, additionally, reduced the export of river water toward the north and northeast into the Arctic basin. Saline Atlantic-derived water thus was replaced by freshwater, which was successively accumulated in the Kara Sea and accordingly imprinted on the stable isotope composition of the bivalve shells. The 1990s freshening in the Kara Sea thus may be caused by natural variations rather than being a signal for global change.

Citation: Simstich, J., I. Harms, M. J. Karcher, H. Erlenkeuser, V. Stanovoy, L. Kodina, D. Bauch, and R. F. Spielhagen (2005), Recent freshening in the Kara Sea (Siberia) recorded by stable isotopes in Arctic bivalve shells, *J. Geophys. Res.*, *110*, C08006, doi:10.1029/2004JC002722.

1. Introduction

[2] Modeling shows that an increased freshwater export from the Arctic Ocean into the northern North Atlantic (see Figure 1 for localities) could induce changes of the Atlantic meridional overturning circulation [*Renssen et al.*, 2001; *Otterå et al.*, 2003; *Saenko et al.*, 2003], which at the end would affect climate of the Northern Hemisphere [*Alley*, 1995]. *Peterson et al.* [2002] argued that the Arctic freshwater content, and thereby its export, may increase owing to the currently observed increase in Siberian river discharge [see also *Bobrovitskaya et al.*, 2003]. *Steele and Ermold* [2004] have shown recently that sea surface salinities in the White Sea and the Kara Sea indeed decreased by 0.4 and 2.9 decade^{-1} since 1980. Increasing river run-off and precipitation can explain the freshening in the White Sea, but not in the Kara Sea, where *Steele and Ermold* [2004] suspect that ice melt/growth and circulation changes may also play a significant role. An example of the mechanisms involved in the response of the sea to changes of sea level pressure and wind fields was given for the Laptev Sea by *Johnson and Polyakov* [2001]. In this case, initially local changes of the freshwater budget caused a salinity increase in the upper layers of large portions of the Arctic Ocean [*Johnson and Polyakov*, 2001]. This example illustrates the importance of hydrographic monitoring the vast Siberian shelf seas for the early detection of climatic/hydrologic changes in the Arctic and the Northern Hemisphere.

[3] Continuous monitoring programs, which could detect hydrological changes, are rare in the Kara Sea. Ship-borne measurements are impossible in periods of sea ice formation

[1]Department of Earth Sciences, University of Cambridge, Cambridge, UK.
[2]Formerly at Leibniz Institute for Marine Sciences (IFM-GEOMAR), Kiel, Germany.
[3]Institute for Oceanography, University of Hamburg, Hamburg, Germany.
[4]Alfred-Wegener-Institute for Polar and Marine Research, Bremerhaven, Germany.
[5]Also at O.A.Sys.–Ocean Atmosphere Systems GbR, Hamburg, Germany.
[6]Leibniz-Laboratory for Radiometric Dating and Stable Isotope Research, Kiel University, Kiel, Germany.
[7]Arctic and Antarctic Research Institute, St. Petersburg, Russia.
[8]Vernadsky Institute of Geochemistry and Analytical Chemistry, Moscow, Russia.
[9]Leibniz Institute for Marine Sciences (IFM-GEOMAR), Kiel, Germany.
[10]Also at Academy of Sciences, Humanities, and Literature, Mainz, Germany.

0148-0227/05/2004JC002722$09.00

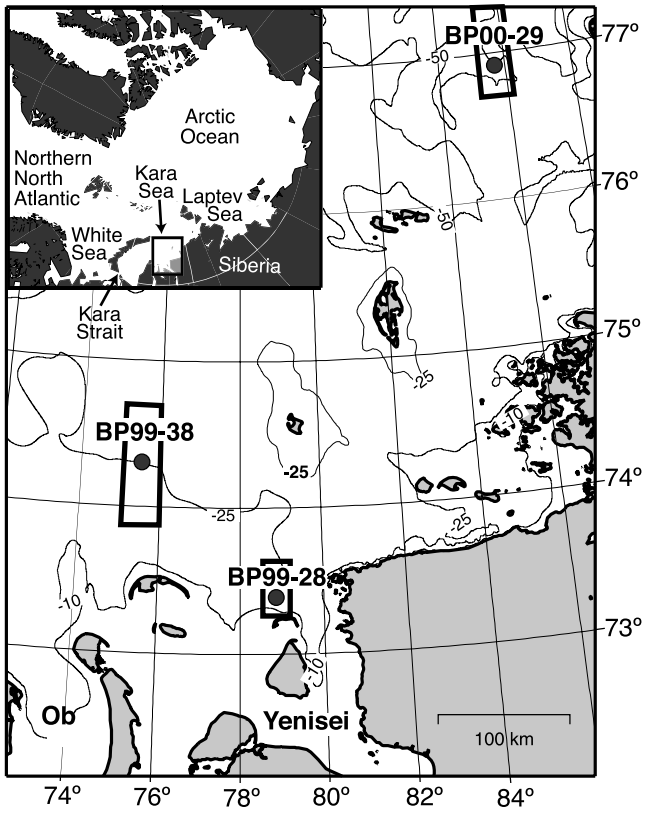

Figure 1. Bivalve sampling sites and boxes for hydrographic data. Inset shows regional setting of the study area (rectangle) in the Arctic.

and breakup, and the risk of losing year-round moorings of CTD (conductivity-temperature-depth) and current meters owing to ice drift and fishing activities is rather high in the shallow shelf waters. Proxy data and modeling provide a possibility to fill this gap. A well-established method to obtain high-resolution records of annual changes in water temperature, salinity, and provenance is provided by stable isotopes in bivalve shells [e.g., *Epstein et al.*, 1953; *Erlenkeuser and Wefer*, 1981; *Arthur et al.*, 1983; *Dettman et al.*, 2004; *Schöne et al.*, 2004]. In Arctic environments, where temperature changes are relatively small, this method appears to be particularly useful for the reconstruction of freshwater variations [*Israelson et al.*, 1994; *Weidman et al.*, 1994; *Khim et al.*, 2001, 2003; *Mueller-Lupp et al.*, 2003; *Simstich et al.*, 2003].

[4] In this work, we combine hydrographic data from direct measurements and modeling to compare with oxygen and stable carbon isotope profiles on bivalve shells from the Kara Sea. The results indicate that the recent freshening trend found at the sea surface by *Steele and Ermold* [2004] is also present at the bottom of the shallow (20 to 70 m water depth) Kara Sea. We address the causes for this local freshening and show how it reflects atmospheric changes on a much larger spatial scale.

2. Methods

[5] In order to determine spatial variability of hydrography, bivalves from three stations in different water depth and distance from the river mouths were chosen (Figure 1, Table 1): a shallow station close to Yenisei estuary (BP99-28, 23 m water depth), a station in intermediate water depth north of Ob estuary (BP99-38, 31 m), and a station in comparatively deep water on the shelf farther north (BP00-29, 73 m).

2.1. Measured Temperature and Salinity From the Hydrographic Database

[6] Modeling and isotope data are referred to temperature and salinity obtained from the hydrographic database of the Arctic and Antarctic Research Institute in St. Petersburg (Russia). These data were measured with deep-sea thermometers, electrical salinity meters, and titration until 1990, and with CTD-probes (Conductivity-Temperature-Depth) afterward. The analytical accuracy of all methods is equal to or better than 0.01° to 0.05°C for temperature and 0.01 for salinity [*Volkov et al.*, 2002]. Data density is irregular over the last 50 years, showing a decreasing number of measurements since 1990. Data from summer are dispersed between the second half of July and beginning of October, and winter data are from March to May. As a reference for bottom water, measurements were taken from the deepest horizons in CTD profiles within defined boxes around the stations under investigation. Salinity is reported without units using the Practical Salinity Scale [*Millero*, 1993].

2.2. Hydrographic Modeling

[7] Modeling of daily mean temperature and salinity was done with the hydrodynamic three-dimensional coupled ice-ocean model HAMSOM/VOM (Hamburg Shelf Ocean Model/Vector Ocean Model) applied to the Kara Sea in 9.4 km horizontal grid resolution [*Backhaus*, 1985; *Harms and Karcher*, 1999; *Harms et al.*, 2000]. The thickness of the depth levels in the model depends on topography. Surface and bottom layers are resolved in 4-m intervals. The model thus provides high resolution in shallow areas such as our sampling sites. The circulation model is coupled to a thermodynamic and dynamic sea ice model [*Hibler*, 1979]. Sea surface heat fluxes are used to determine prognostically ocean temperature and ice formation [*Parkinson and Washington*, 1979; *Maykut*, 1986]. Salt fluxes due to brine and freshwater release are proportional to thermodynamic ice growth.

[8] Atmospheric forcing for the model comes from the NCEP database (www.ncep.noaa.gov). River runoff data

Table 1. Sampling Sites, Dates, and Species

Station	Latitude	Longitude	Depth	Date	Species
BP00-29	76.94°N	85.76°E	73 m	16 September 2000	*Astarte borealis* (Schumacher 1817)
BP99-38	74.25°N	75.61°E	31 m	07 September 1999	*Astarte borealis* (Schumacher 1817)
BP99-28	73.42°N	78.81°E	23 m	04 September 1999	*Serripes groenlandicus* (Bruguière 1789)

were taken from the R_ArcticNET database (www.r-arcticnet.sr.unh.edu). Amplitudes and phases for tides were taken from tidal models of the Arctic Ocean [*Gjevik and Straume*, 1989; *Kowalik and Proshutinsky*, 1993]. At open boundaries, sea surface elevations are prescribed as tidal elevations, the long-term far field sea surface variability (only for the Kara Strait; see Figure 1), and a baroclinic adjustment for horizontal density gradients. Volume flux through the Kara Strait was taken from the larger-scale coupled ice-ocean general circulation model NAOSIM (North Atlantic/Arctic Ocean-Sea Ice Model) [*Karcher et al.*, 2003]. The HAMSOM/VOM simulation of the period 1996 to 2002 was started in September 1995 using initial conditions from previous climatological simulations [*Harms et al.*, 2003]. The climatological spin-up was run for 3 years in full prognostic mode in order to achieve a cyclic stationary state [*Harms and Karcher*, 2005]. Temperature and salinity time series for the near-bottom layer of each of the three stations under investigation were extracted after the model run.

2.3. Stable Isotope Records From Bivalve Shells

[9] Living bivalves of the species *Astarte borealis* and *Serripes groenlandicus* were obtained by dredging the sediment surface on two expeditions with R/V *Akademik Boris Petrov*, in summer 1999 and 2000 (Table 1) [*Stein and Stepanets*, 2000; *Stein and Stepanets*, 2001]. Both species are adapted to cold, boreal-arctic waters (down to −2°C); they are living infaunal by filtering food particles through a siphon from the bottom water [*Gordillo and Aitken*, 2000]. *A. borealis* requires a minimum salinity of 15, whereas *S. groenlandicus* is a euryhaline species [*Gordillo and Aitken*, 2000].

[10] The bivalves were either drowned in ethanol (BP99-28 and BP99−38) or boiled for 2 min in ship tap water (BP00-29). The shell surfaces were cleaned carefully with a brush. They were rinsed with de-ionized water, and dried at 60°C. For isotope analysis, sample carbonate was slowly milled with a dentist drill (0.2-mm carbide finishing bur, Orthodontics-DMI-AG) from the shell's surface as short 5- to 10-mm-long tracks, ∼0.2 mm deep, positioned every 0.3 to 0.5 mm transverse to the (imaginary) central sampling line, parallel to the growth rings (Figure 2). Sample positions are reported as "shell height" measured as rectified distance on the shell from the umbo in growth direction.

[11] Oxygen and stable carbon isotope compositions were measured on a Finnigan MAT 251 mass spectrometer with an automated Carbo-Kiel preparation line (Kiel Device I) at the Leibniz Laboratory of Kiel University. The $^{18}O/^{16}O$ and $^{13}C/^{12}C$ isotope ratios of carbonate samples are reported in the usual δ notation as $\delta^{18}O$ and $\delta^{13}C$, respectively [*Rye and Sommer*, 1980], versus the Peedee Belemnite (PDB) scale established via the NBS 20 (National Bureau of Standards) carbonate stable isotope standard. The analytical error is ±0.07‰ for $\delta^{18}O$ and ±0.04‰ for $\delta^{13}C$. Additional isotope analyses on subsets of samples next to the central sampling line showed that the isotope curves are reproducible [*Simstich et al.*, 2003]. All carbonate isotope data are available via www.pangaea.de.

2.4. Calculation of Expected Equilibrium $\delta^{18}O$

[12] X-ray diffraction proved the bivalve shells to consist completely of aragonite [see also *Khim et al.*, 2003; *Mueller-Lupp et al.*, 2003]. Aragonite $\delta^{18}O$ values ($\delta^{18}O_{exp}$) are expected to be precipitated in thermodynamic equilibrium at temperature *T* with the oxygen isotope composition of the ambient water according to the following equation (modified from *Böhm et al.* [2000]:

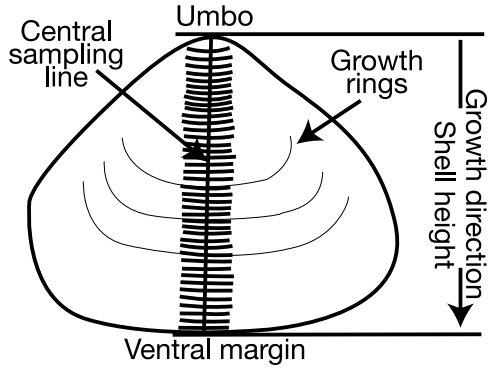

Figure 2. Scheme of sampling on the bivalve shells.

$$\delta^{18}O_{exp} = 4.52 - 0.23\ T + \delta_w, \quad (1)$$

where δ_w measures the isotopic composition of water [*Rye and Sommer*, 1980]. Equation (1) updates the widely used original equation of *Grossman and Ku* [1986]. It includes the data of *Grossman and Ku* [1986], *Rahimpour-Bonab et al.* [1997], and *Tarutani et al.* [1969] and was defined for temperatures ranging from 3° to 28°C [*Böhm et al.*, 2000]. We extrapolate beyond this temperature range, because the bivalves of this study lived at an average temperature of −1.4°C. At this temperature, the $\delta^{18}O$ of aragonite is assumed to be close to equilibrium owing to a slow precipitation rate [*Zhou and Zheng*, 2003].

[13] Conversion of the $^{18}O/^{16}O$-composition of water on the V-SMOW scale (Vienna-Standard Mean Ocean Water; $\delta^{18}O_{water}$) to δ_w, follows [*Hut*, 1987]:

$$\delta_w = 0.99973 \cdot \delta^{18}O_{water,V-SMOW} - 0.27‰. \quad (2)$$

[14] The $\delta^{18}O_{water}$ is calculated from salinity (*S*) following a relationship deduced from bottom water samples of the Kara Sea (Figure 3a) [*Bauch et al.*, 2003; *Simstich et al.*, 2004]:

Salinity ≤ 30

$$\delta^{18}O_{water} = -17.9 + 0.47\ S \qquad \left(r^2 = 0.98, n = 11\right) \quad (3)$$

Salinity > 30

$$\delta^{18}O_{water} = -26.5 + 0.76\ S \qquad \left(r^2 = 0.92, n = 24\right). \quad (4)$$

The relationship between salinity and $\delta^{18}O_{water}$ at the bottom of the Kara Sea is not linear between the two end-members river water and Atlantic Water. Sea ice formation contributes brine waters with high salinity but low $\delta^{18}O$ values as a third component to the bottom waters, thus skewing the $\delta^{18}O_{water}$/salinity regression to the right (Figure 3a) [*Craig and Gordon*, 1965; *Bauch et al.*, 2005]. The regression lines intersect close to salinity = 30.

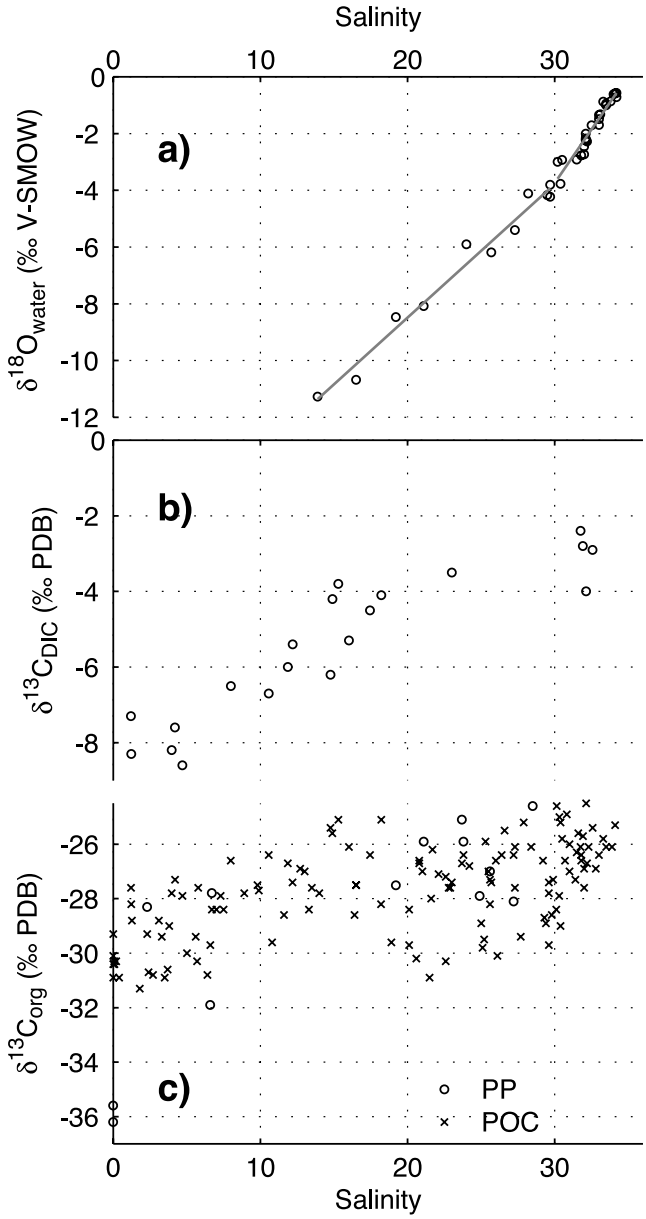

Figure 3. Results of isotopic measurements on samples from the water column versus salinity: a) $\delta^{18}O$ of bottom water, b) $\delta^{13}C$ of dissolved inorganic carbon (DIC), and c) $\delta^{13}C$ of particulate organic carbon (POC) and phytoplankton (PP) (see *Kodina et al.* [1999], *Kodina and Bogacheva* [2002], *Erlenkeuser et al.* [2003], and *Simstich et al.* [2004] for sampling and measuring details).

2.5. Expectation for $\delta^{13}C$ in Bivalves

[15] According to *McConnaughey et al.* [1997], the expected carbon isotope composition in bivalve shells ($\delta^{13}C_{exp}$) depends on $\delta^{13}C$ of environmental carbon ($\delta^{13}C_{env}$) and a certain fraction (R) of respired metabolically derived carbon ($\delta^{13}C_{resp}$):

$$\delta^{13}C_{exp} - \Delta = R \cdot \delta^{13}C_{resp} + (1 - R) \cdot \delta^{13}C_{env}, \qquad (5)$$

where Δ is the equilibrium fractionation between HCO_3^- of the bivalve's organic tissue and its aragonitic shell. R may be between 10% [*McConnaughey et al.*, 1997] and 50% [*Tanaka et al.*, 1986] and may change in relation to metabolic activity [*Klein et al.*, 1996; *Owen et al.*, 2002]. The $\delta^{13}C_{resp}$ derives from $\delta^{13}C$ of the bivalve's food [*McConnaughey et al.*, 1997], mainly particulate organic carbon (POC) [*Wotton*, 1990]. The $\delta^{13}C_{POC}$, and $\delta^{13}C$ of phytoplankton alike (Figure 3c), is about 20 to 24‰ lower than $\delta^{13}C$ of the dissolved inorganic carbon in the water ($\delta^{13}C_{DIC}$, Figure 3b), which represents $\delta^{13}C_{env}$ in equation (5). Low isotope ratios of both, organic and inorganic carbon are tied to low salinity [see also *Erlenkeuser et al.*, 1999, 2003], and reflect the admixture of isotopically light carbon from terrestrial sources to the Kara Sea through the riverine waters. The carbon isotope records of the bivalve shells are therefore expected to covary widely with the oxygen isotope records, but may exhibit an additional lowering in the presence of ^{13}C-depleted organic carbon.

3. Results

3.1. Temperature and Salinity Records

[16] Average bottom water temperature and salinity (T/S) values and data ranges in both hydrographic data sets, measured (Figure 4) and modeled (Figure 5), strongly vary with water depth and distance from the river mouths. Average temperature is higher and average salinity is lower at the shallow river-proximal station BP99-28 than at BP00-29 in the deeper water to the north. T/S data cover significantly wider ranges in shallower than in deeper water, indicating that bottom water in 20 to 30 m depth is more changeable than in 70 m.

[17] Most temperature and salinity values measured in winter lie within the ranges of T/S measurements in summer (Figure 4). Conversely, the modeling data suggest certain seasonal cycles between low temperature/high salinity in winter and high temperature/low salinity in summer (Figure 5). Interannual variability seems to be higher for summers than for winters, and higher in shallower than in deeper water. The most extreme T/S values of each winter form baselines from which temperatures increase and salinities decrease dramatically in late spring/early summer during river spring flood and sea ice melt. Full summer values in the model are mostly reached by an initially small increase of 0.2° to 0.5°C (salinity: 2 to 5) followed by a more pronounced rise of <0.5° to 4°C (S: 2 to 8), then finally a rapid return to winter conditions.

[18] The winter baselines of salinity at all stations reveal trends toward lower salinity over the years 1996 to 2001 (Figure 5 and Table 2). These trends are clearly defined at the two shallow, river-proximal sites BP99-28 and BP99-38 (-0.2 yr^{-1}), and less defined at the deep station BP00-29 (-0.008 yr^{-1}). Temperature trends are not distinguished. Trends in the T/S data obtained by measurements (Figure 4) are not considered significant because the measurements do not form continuous time series.

3.2. Expected and Measured Isotope Records

[19] Conversion of bottom T/S obtained by modeling into oxygen isotope series as expected to be found along the bivalve shells ($\delta^{18}O_{exp}$, equations (1) to (4)) reveals cyclic changes with highest values during late winter/early spring and dramatically decreasing values in late spring/early

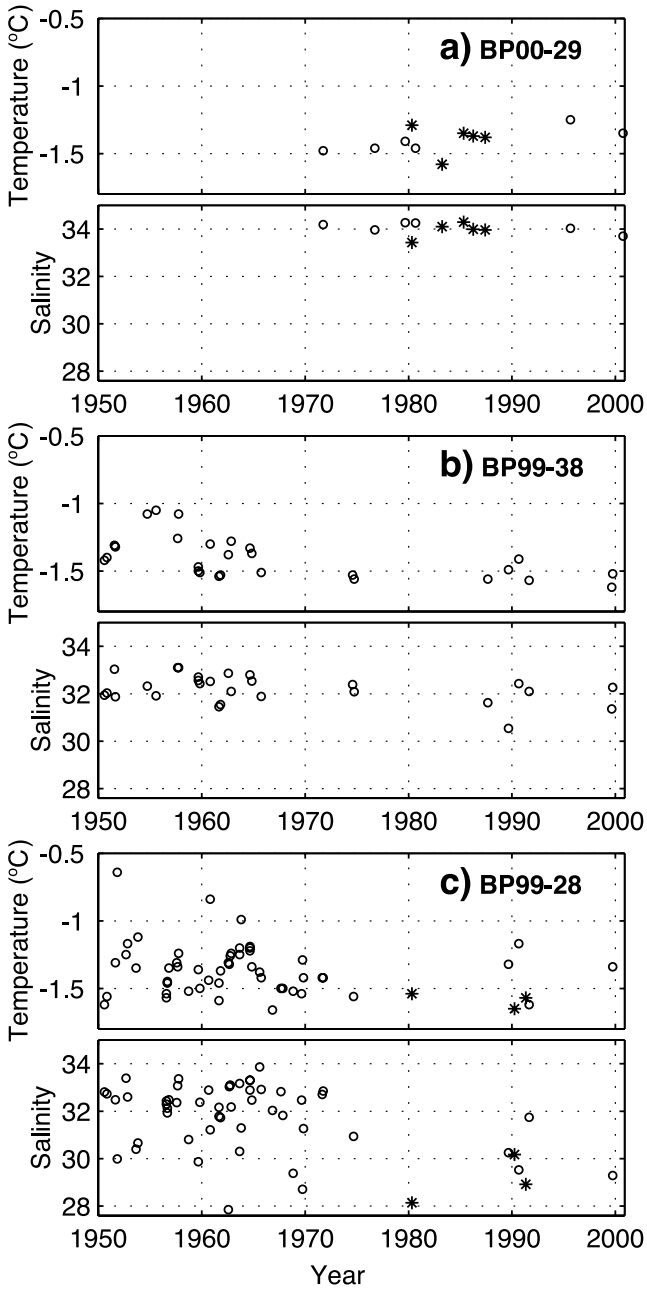

Figure 4. Near-bottom (top) temperature and (bottom) salinity from CTD measurements in the boxes around the sampling sites (Figure 1). Circles, summer (July to September/October); stars, winter (March to May).

summer (Figure 6). Thus $\delta^{18}O$ in the bivalves is expected to show the same pattern, i.e., to mirror summer freshening and warming of the bottom water. Seasonal $\delta^{18}O$ differences are expected to be higher in shallower than in deeper water, in close similarity to the hydrographic data. Moreover, peak summer values should show higher interannual variability than peak winter values, and this interannual variability is expected to be higher in shallower than in deeper water (Figure 6). Regression lines through the peak winter values in the modeled data series reveal negative trends of around -0.1‰ yr^{-1} at the two shallow stations, and -0.01‰ yr^{-1} at the deep station BP00-29 (Figure 6 and Table 2).

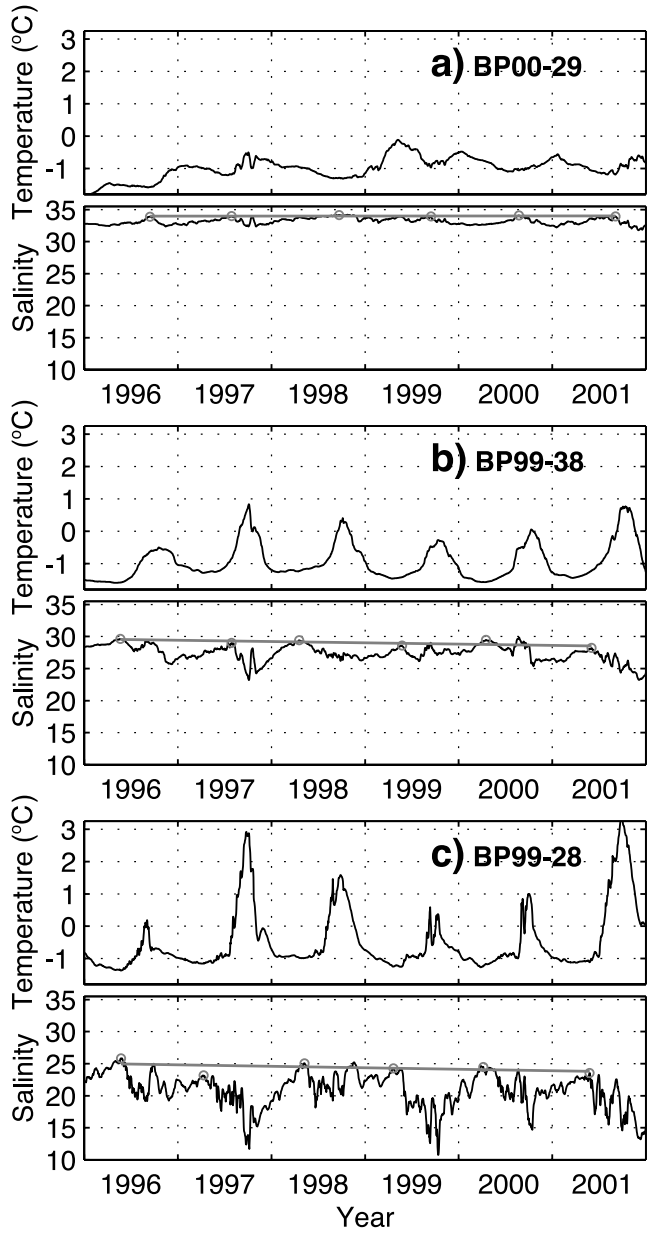

Figure 5. (top) Temperature and (bottom) salinity of the bottom water near the sampling locations obtained by modeling. Open circles denote highest salinity of each year. Straight lines are regression lines through these points.

[20] The actual isotope measurements on the bivalve shells ($\delta^{18}O_{biv}$ and $\delta^{13}C_{biv}$, Figure 7) revealed patterns, which confirm the important characteristics of the $\delta^{18}O_{exp}$ curves obtained by modeling: Average values are lower and

Table 2. Trends in the Salinity (S) and Isotope Records of Figures 5 to 7

Station	Depth	S, yr^{-1}	$\delta^{18}O_{exp}$, ‰ yr^{-1}	$\delta^{18}O_{biv}$, ‰ yr^{-1}	$\delta^{13}C_{biv}$, ‰ yr^{-1}
BP00-29	73 m	−0.008	−0.01	−0.07	−0.008
BP99-38	31 m	−0.2	−0.09	−0.09	−0.15
BP99-28	23 m	−0.2	−0.11	−0.17	−0.26

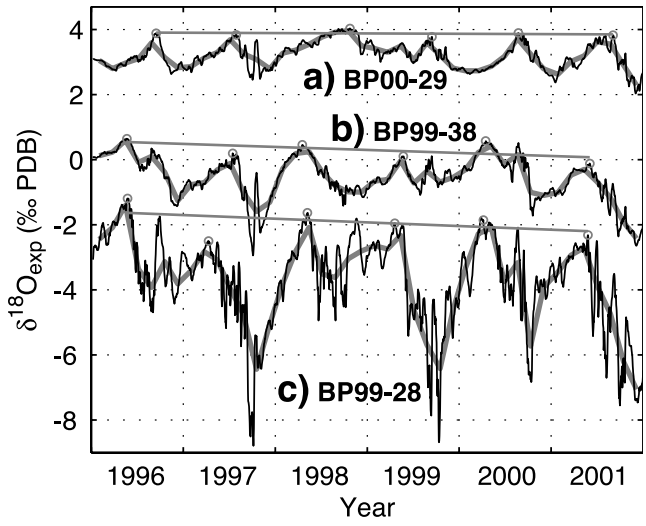

Figure 6. Expected $\delta^{18}O$ calculated by applying equations (1) to (4) to bottom water temperature and salinity obtained by modeling (Figure 5). Open circles denote peak winter values. Straight lines are regression lines through these points. Thick shaded lines illustrate possible smoothing of the $\delta^{18}O_{exp}$ curves resulting from the sampling strategy.

the data ranges are higher in shallow than in deeper water. Most of the variability is due to the peak low values, which are more variable than the peak high values.

[21] In order to define trends in the bivalves' isotope records, we divided them in consecutive years using the oscillations between higher and lower values as stratigraphic markers. Most yearly cycles begin and end with co-occurring high $\delta^{18}O_{biv}$ and $\delta^{13}C_{biv}$ values, defined as indicative of winter periods when ^{18}O- and ^{13}C-enriched water dominates the bottom layer in the Kara Sea. Typically, a yearly cycle (e.g., 10.5 to 14 mm in Figure 7b) starts with a slow $\delta^{18}O$ decrease, which accelerates afterward and ends in one or more very light values, later increasing rapidly to a new maximum from which the cycle starts again. These cycles clearly reflect ^{18}O-depleted and generally warmer river water (Figures 5 and 6), which starts to accumulate below the fast ice in early spring, and becomes the dominant water mass in late spring/early summer [*Macdonald*, 2000]. During the slow $\delta^{18}O$ decrease, the corresponding $\delta^{13}C$ record usually shows a first minimum and a second minimum when $\delta^{18}O$ is near its lowermost point in the cycle. The negative $\delta^{13}C$ peaks mirror the uptake of ^{13}C-depleted inorganic carbon supplied by the river water in combination with the uptake of ^{13}C-depleted organic carbon following two algae blooms. The first bloom happens in spring as soon as the rising sunlight penetrates the ice cover [*Grebmeier et al.*, 1995]. A second bloom in summer is triggered by the increasing supply of river water and its nutrients [*Pivovarov et al.*, 2003]. Preferential uptake of ^{12}C by the algae and its vertical export leads to an increased availability of ^{12}C enriched, i.e., ^{13}C-depleted particulate organic carbon at the bottom [*Michener and Schell*, 1994].

[22] Six to nine complete yearly cycles could be detected in the bivalve records of the shallower stations BP99-28 and BP99-38 (Figures 7b and 7c). Regression lines defined by the high winter values in $\delta^{18}O_{biv}$ reveal negative trends of -0.17 and -0.09‰ yr^{-1}, similar to the trends in the corresponding $\delta^{18}O_{exp}$ series (Figure 6 and Table 2). The $\delta^{13}C_{biv}$ also shows negative trends of similar magnitude (-0.26 and -0.15‰ yr^{-1}). Allowing for uncertainties in

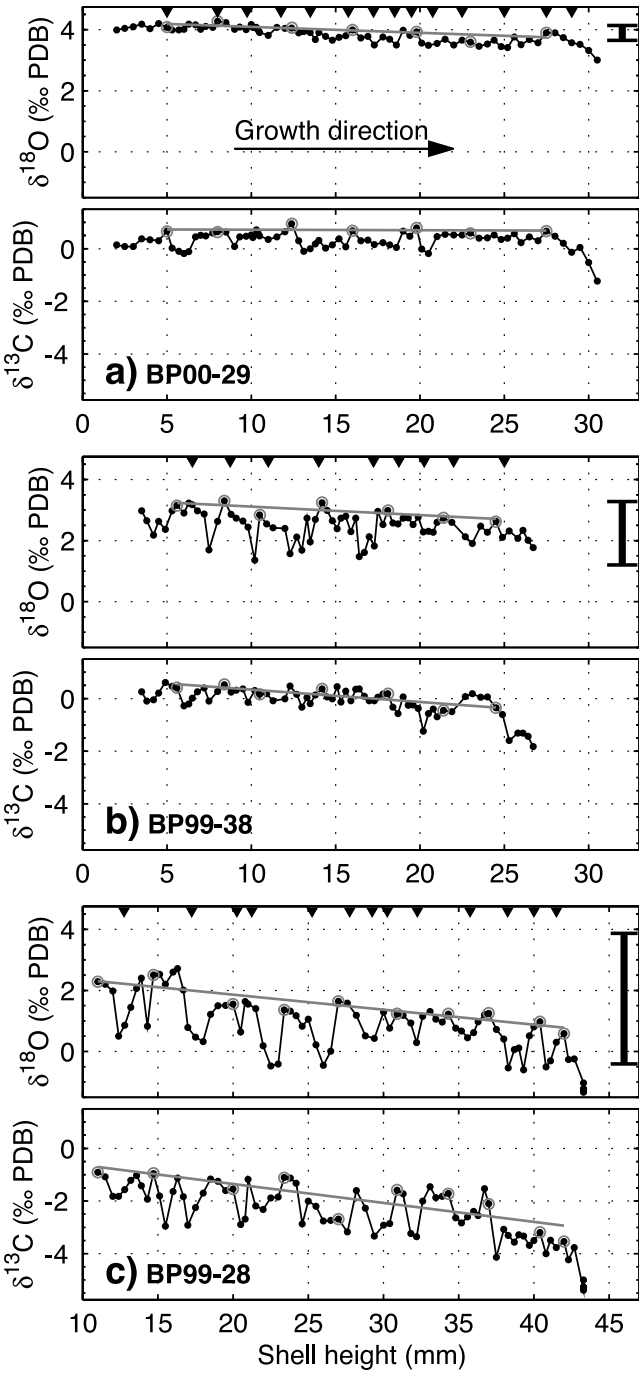

Figure 7. (top) The $\delta^{18}O$ and (bottom) $\delta^{13}C$ records of the bivalves. Open circles denote defined peak winter values. Straight lines are regression lines through these points. Small triangles on top show position of growth rings on the shell surfaces. Vertical lines to the right show expected $\delta^{18}O_{exp}$ data ranges for the bottom water calculated by applying equations (1) to (4) to the data ranges of temperature and salinity from the hydrographic database (Figure 4).

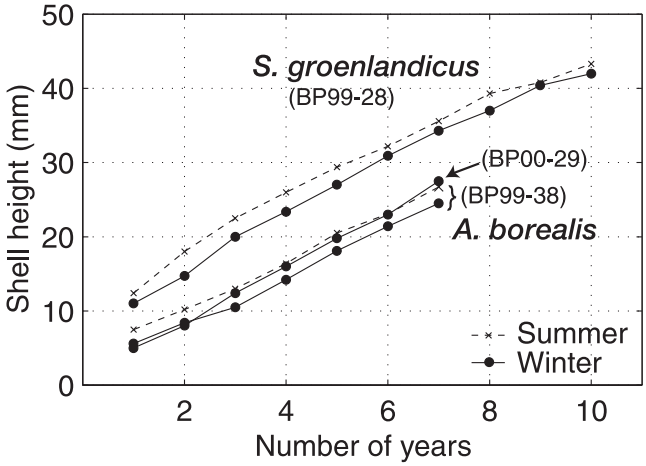

Figure 8. Growth rates of the bivalves as received from defining years according to the isotope cycles defined in Figure 7.

defining the yearly increments in some parts of the shells (for example, 21 mm instead of 20 mm in Figure 7c) does not seriously change the trends. For *A. borealis* at the deep station BP00-29, seasonal cycles are too cryptic to enable simple definition of years (Figure 7a). At this station, trends were tentatively estimated by assuming an average growth rate of ~3.5 mm yr^{-1} as shown by *A. borealis* at station BP99-38 (Figures 7b and 8). Selecting the highest co-occurring $\delta^{18}O$ and $\delta^{13}C$ values at roughly every 3.5 mm reveals trends of −0.07‰ $\delta^{18}O$ yr^{-1} and −0.008‰ $\delta^{13}C$ yr^{-1} at BP00-29 (Figure 7a).

4. Discussion

4.1. Effects of Sampling Strategies on Data Ranges and Average Values

[23] The ranges of the $\delta^{18}O_{exp}$ values, expected from measured bottom temperature and salinity (Figure 4), generally match with the ranges of $\delta^{18}O_{biv}$ measured on the bivalve shells (Figure 7). However, both $\delta^{18}O_{exp}$ from measured T/S and $\delta^{18}O_{biv}$ are 1 to 6‰ higher and cover 3 times smaller ranges than the corresponding $\delta^{18}O_{exp}$ series derived from modeling (Figure 6). This general disagreement is rooted in the T/S data, because the salinities from modeling (Figures 5b and 5c) are generally lower, and peak temperatures higher, than from measurements (Figures 4b and 4c). These mismatches reflect differences in the data collection. The combined effects of data gridding and spatial resolution in the model may bias bottom water properties slightly toward surface values. The agreement between modeled and measured data ranges may further suffer from the much lower time resolution of the CTD measurements, which may miss the enormously high and short-termed hydrographic variability at the bottom of the shallow Kara Sea. Especially, the lowest salinities during run-off peaks are easily missed out by measurements, because of the inaccessibility of the area during these times.

[24] The mismatches between modeled and measured data are not considered to affect the negative salinity trends found in the modeling data, because these are robust in the Kara Sea modeling domain as a whole (see below). Additional support comes from *Steele and Ermold* [2004], who recently reviewed observational data and found a salinity trend of −2.9 $decade^{-1}$ since 1980.

[25] Another cause for the disagreement between measured and modeled data may result from the sampling procedure for the isotope records on the bivalve shells, which probably fail to cover the true isotope ranges fully. On average, seven samples per year were analyzed, which gives a time resolution of ~52 days/sample (Figure 9). Additionally, the milling procedure resulted in a truncated sinusoid profile for each single sample, because more material was scraped off the shell directly at the tip of the drill than at its side, hence overemphasizing values in the middle of the 52-day intervals. Figure 9 shows an example of how this sampling procedure theoretically lowers the data range if the drill tip is centered on high $\delta^{18}O_{exp}$ values of approximately −0.4‰ in October 1997 surrounded by much lower values with peaks of −2.9 to −2.2‰ in the days before and after. The resulting measurement would give −1.6‰. Considering this effect, all $\delta^{18}O_{biv}$ curves are only smoothed images of the underlying natural $\delta^{18}O$ variability. Smoothing would mostly affect the summer extremes because of their short-term character, but could also affect the winter signature, if winter growth of the bivalves is much reduced. However, the isotope profiles along the shells show broad winter peaks and hence provide a reliable basis for quantifying trends in the winter isotope composition. How the smoothing affects the whole records is illustrated by the thick shaded lines in Figure 6, which also reveal the trends in the $\delta^{18}O$ records to be consistent despite smoothing, and not a product of sampling strategy.

4.2. Biological Bias

[26] Different environmental parameters, for example, temperature, salinity, and food supply, control the rate and timing of shell growth in bivalves [e.g., *Andrews*, 1972; *Tallqvist and Sundet*, 2000; *Schöne et al.*, 2003]. Enhanced growth rates generally lower the oxygen and carbon isotope ratios in biologically precipitated carbonates owing to kinetic fractionation [*McConnaughey*, 1989; *McConnaughey et al.*, 1997]. An additional metabolic

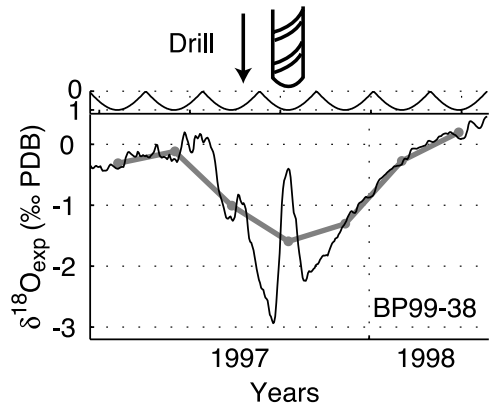

Figure 9. Scheme illustrating the smoothing (thick shaded curve) of an original $\delta^{18}O_{exp}$ curve (thin black curve) by sampling with a dentist's drill. Top curve is sinusoid used to calculate weighted average (thick shaded dots) of the original $\delta^{18}O_{exp}$ data.

effect due to an increased uptake of respired carbon provokes further reduction of the shells' $\delta^{13}C$ [*Klein et al.*, 1996; *Owen et al.*, 2002]. Enhanced growth rates in conformity with the generally higher biological activity during Arctic summers [*Grebmeier et al.*, 1995] thus could induce an additional lowering of already low $\delta^{18}O$ and $\delta^{13}C$ summer peaks in the bivalves' isotope records.

[27] Growth deceleration, on the other hand, would reduce the obtainable sample resolution and limit reconstructions of the full seasonal range from bivalve shells [e.g., *Wilkinson and Ivany*, 2002; *Ivany et al.*, 2003]. *Goodwin et al.* [2003] illustrate that a growth shutdown during either winter or summer results in saw-toothed patterns in bivalve isotope curves. Negative trends over winter values, as observed in our records (Figure 7), could only be produced, if at all, by a regular winter shutdown, which steadily prolongs over the bivalve's lifetime [*Goodwin et al.*, 2003] [see also *Harrington*, 1989]. No such growth changes are evident from our specimens.

[28] Direct observations of shell growth are not available for *A. borealis* and *S. groenlandicus*. Growth thickenings on the shell surface cannot be used to determine growth rates, because only some of the growth rings on *S. groenlandicus* match annual cycles, but some hardly show coherence (Figure 7c). Growth rings of *A. borealis* are found to be totally unrelated to annual cycles [*Mueller-Lupp et al.*, 2003]. This is in accordance with previous findings that growth rings do not generally indicate yearly markers, but can develop owing to, for example, disturbance by storms or predators [*Andrews*, 1972; *Lutz and Rhoads*, 1980; *Jones*, 1981].

[29] However, *Khim et al.* [2001] reported a good correspondence between internal growth structures and $\delta^{18}O$ cycles in shells of *S. groenlandicus*, although our own experiments on stained thin sections [cf. *Schöne et al.*, 2004] did not disclose growth increments. *Khim et al.* [2001] also showed that the isotope cycles of *S. groenlandicus* match annual hydrographic cycles. The same was shown for *A. borealis* in the Laptev Sea [*Mueller-Lupp et al.*, 2003] and for many other species in different areas [e.g., *Dettman et al.*, 2004; *Schöne et al.*, 2004; *Immenhauser et al.*, 2005]. The bivalves' isotope cycles thus are considered to be suitable for the determination of yearly growth increments. This approach yielded average annual growth rates of 3.1 to 3.8 mm yr^{-1} (Figure 8), which are close to growth rates reported in literature, for example, 1.7–3.0 mm/yr for *Astarte borealis* in the Laptev Sea [*Mueller-Lupp et al.*, 2003], and 4.3–6.5 mm/yr and 5.5–12 mm/yr for *Serripes groenlandicus* in the Canadian Arctic [*Andrews*, 1972] and the Bering Strait area [*Khim et al.*, 2003], respectively.

[30] Figure 8 excludes any major changes in growth rates during the bivalves' lifetimes. This finding argues against a lengthening of winter growth shutdown with shell age to be the cause for the isotopic trends [*Goodwin et al.*, 2003]. Moreover, winter $\delta^{18}O_{biv}$ and $\delta^{13}C_{biv}$ values in our records form plateaus rather than saw teeth (Figure 7), thus arguing against a winter shutdown at all. Instead, the bivalves appear to continue their growth at winter temperatures, which are not much different from summer (Figure 4). Food my be provided in the bottom nepheloid layer, which probably exists the whole year round as shown for a similar setting in the adjacent Laptev Sea [*Wegner et al.*, 2003]. The obvious saw-toothed patterns of the summer values, on the other hand, more likely reflect the saw-toothed character of the short freshening events (Figure 5) rather than of shell growth behavior.

[31] An additional argument against ontogenetic reasons for the observed trends is that no clear trends are found in isotope records measured on *Serripes groenlandicus* from the Chukchi Sea and the Bering Strait region [*Khim et al.*, 2001, 2003], and on *Astarte borealis* from the Laptev Sea [*Mueller-Lupp et al.*, 2003] and the Scoresby Sund in East Greenland [*Israelson et al.*, 1994]. Ontogenetic trends are obviously not the rule for these species. The very low values at the marginal end of the $\delta^{13}C_{biv}$ records (Figure 7) are yet unexplained [see also *Mueller-Lupp et al.*, 2003]. However, because only the last summer is affected, the long-term trends through the peak winter values will not be concerned. In summary, these isotope trends seem to record changes in the environment rather than changes in growth.

4.3. Causes for the Observed Trends in the Bottom Water

[32] As the bivalves' $\delta^{18}O$ and $\delta^{13}C$ both reveal negative trends, we hypothesize that they are caused by a successively larger fraction of ^{18}O and ^{13}C depleted river water accumulating in the bottom layer of the Kara Sea. By neglecting temperature changes and applying equations (3) and (4), the $\delta^{18}O_{biv}$ trends of Table 2 translate to salinity trends between -0.09 and -0.36 yr^{-1}, with a mean of 0.2 yr^{-1} (± 0.10, n = 6). This corresponds to the trends in the bottom water salinity obtained by modeling (-0.008 to -0.2 yr^{-1}, Table 2) and matches the trends of sea surface salinity of -0.29 yr^{-1} since 1980 found by *Steele and Ermold* [2004]. Mean salinity of the whole Kara Sea model domain (surface to bottom) dropped by roughly 0.5 between 1996 and 2000 (Figure 10c). The locally observed trends at the bottom (Figures 5 to 7) therefore mirror the overall trend. A small contribution to this trend probably derives from the increase in the river discharge (Figure 10e), which, however, in 1996 to 2000 was far below the range of $\sim$25% yr^{-1} required to produce a widespread freshening as simulated in the model [see also *Steele and Ermold*, 2004]. An increased supply of river water to the Kara Sea can thus be ruled out as a single cause for the observed freshening.

[33] More than on river run-off variability, the freshwater balance in the shallow part of the Kara Sea depends on the variability of the inflow of saline Atlantic-derived waters, primarily through the Kara Strait in the southwest (Figure 1), and the export of river water toward the north and northeast into the Arctic basin. The inflow from the southwest is shallow enough to affect the shallow Kara Sea shelf, whereas inflowing Atlantic Water from the north stays in the deep northwestern troughs [*Pavlov and Pfirman*, 1995; *Schauer et al.*, 2002]. The Kara Strait inflow is mainly wind driven [*Harms and Karcher*, 1999]. It decreased steadily during the 1990s, and even reversed in 1999 (Figure 10b) [*Harms and Karcher*, 2005]. The inflow reduction followed the weakening of the prevailing southwesterly winds due to a lowering of the zonal pressure gradients over the Kara Sea during the 1990s. This is indicated by the decrease of the Arctic oscillation index after a record high in 1989 (Figure 10a) [*Thompson and Wallace*, 2000].

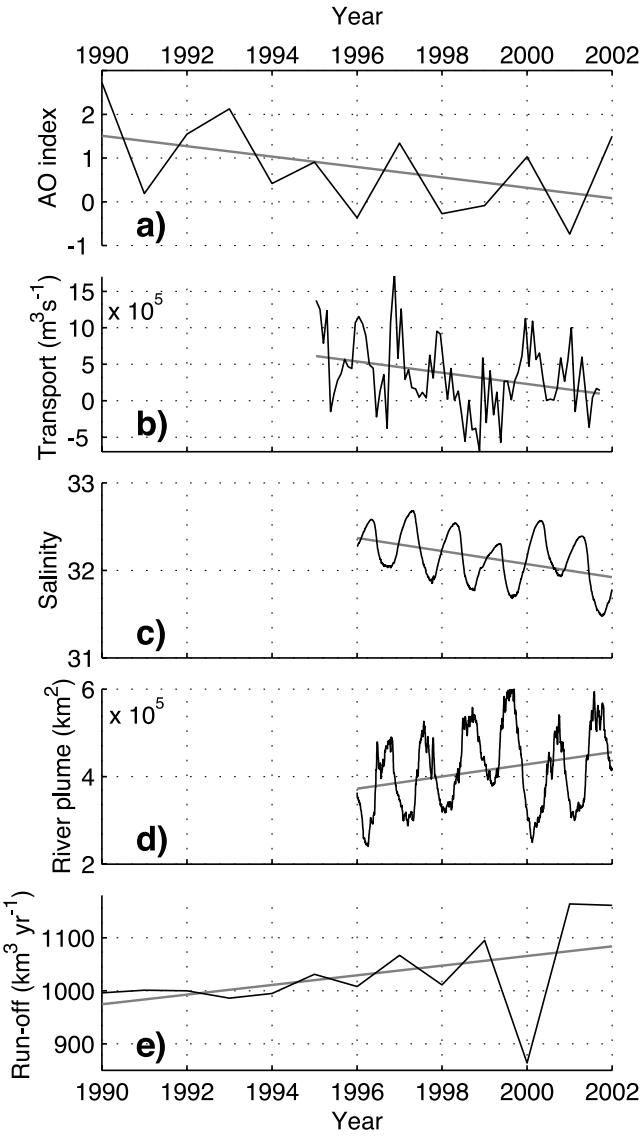

Figure 10. Time series and trends (straight shaded lines) of (a) January to March means of the standardized daily Arctic oscillation (AO) index [*Thompson and Wallace*, 2000], (b) Kara Strait inflow as derived from the AWI/NAOSIM model, (c) mean salinity in the Kara Sea model domain (surface to bottom), and (d) area of the low salinity (<30) plume in the upper 4 m of the Kara Sea model domain as derived from the HAMSOM/VOM model. (e) Combined annual river run-off of Ob and Yenisei (www.r-arcticnet.sr.unh.edu).

[34] The shift of the Arctic oscillation regime also affected the dispersion pathways of river water in the Kara Sea. The weakening of the southwesterly winds significantly reduced the export of river water toward the Arctic basin [*Harms and Karcher*, 2005], thus shifting the relation of Atlantic-derived saline water to river water in favor of the latter. As a result, the extent of low-saline surface waters (i.e., the river plume) increased successively during the late 1990s (Figure 10d). This process enlarged the relative amount of freshwater in the Kara Sea and reduced average salinity, accordingly (Figure 10c). An additional effect may come from a reduction of sea ice production and corresponding brine release into the bottom water due to the changing wind regime [cf. *Winsor and Chapman*, 2002; *Divine et al.*, 2004]. Modeling results, however, showed no significance for this process.

[35] Since both processes, the reduced import of salt and the diminished freshwater dispersion to the northeast, are atmospherically driven, the changes are most pronounced at the sea surface. However, bivalves as benthic animals evidently cannot record surface variability directly. Additionally, a very strong haline stratification in the shallow Kara Sea impedes the direct vertical transfer of water [*Pivovarov et al.*, 2003] and therefore information about surface conditions in form of isotope proxies. Bottom water changes at the sampling sites therefore depend on sporadic countercurrents, which move waters laterally from central and deeper parts of the Kara Sea toward the river mouths [*Dmitrenko et al.*, 2001; *Harms et al.*, 2003]. The source of this water is the main branch of Atlantic-derived inflow crossing the Kara Sea from the Kara Strait toward the northeast [*Harms and Karcher*, 1999; *Harms et al.*, 2000]. Owing to the wind regime changes, the water transported in these countercurrents became effectively less saline during the 1990s as is recorded in the bivalve shells.

5. Conclusions

[36] Changing river water supply from Ob and Yenisei is the main cause for high seasonal hydrographic variability in the bottom water of the shallow Kara Sea as shown by CTD measurements and modeling. Superimposed on the annual cycles of the salinity time series obtained by modeling are negative trends in the winter values, which indicate a substantial and long-lasting freshening during the second half of the 1990s. Isotope cycles along the growth direction of bivalve shells reliably record all aspects of the seasonal bottom water hydrography. Low-resolution isotope sampling may lead to an underestimation of the full extent of the seasonal cycles, while effects from growth rate changes likely are not significant. The bivalves' $\delta^{18}O$ and $\delta^{13}C$ records show negative trends, which indicate successively accumulating ^{18}O and ^{13}C depleted river water in the Kara Sea bottom water.

[37] The measured increase of river run-off during the 1990s was not sufficient as the sole cause for the widespread freshening. Instead, the decreasing Arctic oscillation index during this period indicates a lowering of zonal pressure gradients in the region, which resulted in a weakening of the prevailing southwesterly winds. The weaker winds reduced the freshwater export to the Arctic basin and the saltwater import from the Barents Sea through the Kara Strait. The result was a successive relative increase of the river water fraction as recorded in the bivalve shells. Freshening of Arctic surface waters in general is found to be an alarming signal for global change [e.g., *Arctic Climate Impact Assessment* (*ACIA*), 2004]. The salinity decrease in the Kara Sea during the 1990s, however, seems to be less the result of changes in the hydrologic cycle owing to greenhouse forcing than the result of natural variations in atmospheric pressure fields.

[38] **Acknowledgments.** We thank Jutta Heinze and Sven Roth for XRD-analysis and interpretation, and Bernhard "Peri" Peregovich for

examining thin sections. We are grateful to Thorsten Kiefer for the conclusive tip. We are obliged to H. Heckt and H. H. Cordt, who took care of the isotope measurements. Comments of two anonymous reviewers helped to improve the manuscript. The German Ministry for Education and Research (BMBF) funded this study as part of the joint Russian-German project "Siberian River Run-off (SIRRO)."

References

Alley, R. B. (1995), Resolved: The Arctic controls global climate change, in *Arctic Oceanography: Marginal Ice Zones and Continental Shelves*, *Coastal Estuarine Stud.*, vol. 49, edited by W. O. Smith Jr. and J. M. Grebmeier, pp. 263–283, AGU, Washington, D. C.

Andrews, J. T. (1972), Recent and fossil growth rates of marine bivalves, Canadian Arctic, and Late-Quaternary Arctic marine environments, *Palaeogeogr. Palaeoclimatol. Palaeoecol.*, *11*, 157–176.

Arctic Climate Impact Assessment (ACIA) (2004), *Impacts of a warming Arctic: Arctic Climate Impact Assessment*, 140 pp., Cambridge Univ. Press, New York.

Arthur, M. A., D. F. Williams, and D. S. Jones (1983), Seasonal temperature-salinity changes and thermocline development in the mid-Atlantic Bight as recorded by the isotopic composition of bivalves, *Geology*, *11*, 655–659.

Backhaus, J. O. (1985), A three-dimensional model for the simulation of shelf sea dynamics, *Dtsch. Hydrogr. Z.*, *38*(4), 165–187.

Bauch, D., H. Erlenkeuser, V. Stanovoy, J. Simstich, and R. Spielhagen (2003), Freshwater distribution and brine waters in the southern Kara Sea in summer 1999 as depicted by $\delta^{18}O$ results, in *Siberian River Run-off in the Kara Sea: Characterisation, Quantification, Variability and Environmental Significance*, *Proc. Mar. Sci.*, vol. 6, edited by R. Stein et al., pp. 73–90, Elsevier, New York.

Bauch, D., H. Erlenkeuser, and N. Andersen (2005), Water mass processes on Arctic shelves as revealed from $\delta^{18}O$ of H_2O, *Global Planet. Change*, in press.

Bobrovitskaya, N. N., A. V. Kokorev, and N. A. Lemeshko (2003), Regional patterns in recent trends in sediment yields of Eurasian and Siberian rivers, *Global Planet. Change*, *39*(1–2), 127–146.

Böhm, F., M. M. Joachimski, W.-C. Dullo, A. Eisenhauer, H. Lehnert, J. Reitner, and G. Wörheide (2000), Oxygen isotope fractionation in marine aragonite of coralline sponges, *Geochim. Cosmochim. Acta*, *64*, 1695–1703.

Craig, H., and L. I. Gordon (1965), Deuterium and oxygen 18 variations in the ocean and the marine atmosphere, in *Symposium on Marine Geochemistry*, pp. 9–130, Univ. of R. I., Kingston.

Dettman, D. L., K. W. Flessa, P. D. Roopnarine, B. R. Schöne, and D. H. Goodwin (2004), The use of oxygen isotope variation in shells of estuarine mollusks as a quantitative record of seasonal and annual Colorado River discharge, *Geochim. Cosmochim. Acta*, *68*, 1253–1263.

Divine, D. V., R. Korsnes, and A. P. Makshtas (2004), Temporal and spatial variation of shore-fast ice in the Kara Sea, *Cont. Shelf Res.*, *24*(15), 1717–1736.

Dmitrenko, I. A., J. A. Hölemann, S. A. Kirillov, C. Wegner, V. A. Gribanov, S. L. Berezovskaya, and H. Kassens (2001), Thermal regime of the Laptev Sea bottom layer and affecting processes (in Russian), *Kriosfera Zemli*, *3*, 40–55.

Epstein, S., R. Buchsbaum, H. A. Lowenstam, and H. C. Urey (1953), Revised carbonate-water isotopic temperature scale, *Geol. Soc. Am. Bull.*, *64*, 1315–1326.

Erlenkeuser, H., and G. Wefer (1981), Seasonal growth of bivalves from Bermuda recorded in their O-18 profiles, *Proceedings of the 4th International Coral Reef Symposium*, vol. 2, edited by E. D. Gomez et al., pp. 643–648, Univ. of Philippines, Manila.

Erlenkeuser, H., R. F. Spielhagen, and E. Taldenkova (1999), Stable isotopes in modern water and bivalve samples from the southern Kara Sea, *Ber. Pol. For. Rep. Polar Res.*, *300*, 80–90.

Erlenkeuser, H., H. H. Cordt, J. Simstich, D. Bauch, and R. Spielhagen (2003), DIC stable carbon isotope pattern in the surface waters of the southern Kara Sea, Sep. 2000, in *Siberian River Run-off in the Kara Sea: Characterisation, Quantification, Variability and Environmental Significance*, *Proc. Mar. Sci.*, vol. 6, edited by R. Stein et al., pp. 91–110, Elsevier, New York.

Gjevik, B., and T. Straume (1989), Model simulations of the M2 and the K1 tides in the Nordic Seas and the Arctic Ocean, *Tellus, Ser. A*, *41*, 73–96.

Goodwin, D. H., B. R. Schöne, and D. L. Dettman (2003), Resolution and fidelity of oxygen isotopes as paleotemperature proxies in bivalve mollusk shells: Models and observation, *Palaios*, *18*(2), 110–125.

Gordillo, S., and A. E. Aitken (2000), Palaeoenvironmental interpretation of Late Quaternary marine molluscan assemblages, Canadian Arctic Archipelago, *Geogr. Phys. Quat.*, *54*(3), 301–315.

Grebmeier, J. M., W. O. Smith, and R. J. Conover (1995), Biological processes on Arctic continental shelves: Ice-ocean-biotic interactions, in *Arctic Oceanography: Marginal Ice Zones and Continental Shelves*, *Coastal Estuarine Stud.*, vol. 49, edited by W. O. Smith and J. M. Grebmeier, pp. 231–261, AGU, Washington, D. C.

Grossman, E. L., and T.-L. Ku (1986), Oxygen and carbon isotope fractionation in biogenic aragonite: Temperature effects, *Chem. Geol.*, *59*, 59–74.

Harms, I. H., and M. J. Karcher (1999), Modeling the seasonal variability of hydrography and circulation in the Kara Sea, *J. Geophys. Res.*, *104*(C6), 13,431–13,448.

Harms, I. H., and M. J. Karcher (2005), Kara Sea freshwater dispersion and export in the late 1990s, *J. Geophys. Res.*, *110*, C08007, doi:10.1029/2004JC002744.

Harms, I. H., M. J. Karcher, and D. Dethleff (2000), Modelling Siberian river runoff: Implications for contaminant transport in the Arctic Ocean, *J. Mar. Syst.*, *27*, 95–115.

Harms, I. H., U. Hübner, J. O. Backhaus, M. Kulakov, V. Stanovoy, O. V. Stepanets, L. A. Kodina, and R. Schlitzer (2003), Salt intrusions in Siberian river estuaries: Observations and model experiments in Ob and Yenisei, in *Siberian River Run-off in the Kara Sea: Characterisation, Quantification, Variability, and Environmental Significance*, *Proc. Mar. Sci.*, vol. 6, edited by R. Stein et al., pp. 27–45, Elsevier, New York.

Harrington, R. J. (1989), Aspects of growth deceleration in bivalves: Clues to understanding the seasonal $\delta^{18}O$ and $\delta^{13}C$ record—A comment on Krantz et al. (1987), *Palaeogeogr. Palaeoclimatol. Palaeoecol.*, *70*, 399–403.

Hibler, W. D., III (1979), A dynamic thermodynamic sea ice model, *J. Phys. Oceanogr.*, *9*, 815–846.

Hut, G. (1987), Consultants' group meeting on stable isotope reference samples for geochemical and hydrological investigations: Report to the Director General, report, 42 pp., Int. Atomic Energy Agency, Vienna.

Immenhauser, A., T. F. Nagler, T. Steuber, and D. Hippler (2005), A critical assessment of mollusk $^{18}O/^{16}O$, Mg/Ca, and $^{44}Ca/^{40}Ca$ ratios as proxies for Cretaceous seawater temperature seasonality, *Palaeogeogr. Palaeoclimatol. Palaeoecol.*, *215*, 221–237.

Israelson, C., B. Buchardt, S. Funder, and H. W. Hubberten (1994), Oxygen and carbon isotope composition of Quaternary bivalve shells as a water mass indicator: Last interglacial and Holocene, East Greenland, *Palaeogeogr. Palaeoclimatol. Palaeoecol.*, *111*, 119–134.

Ivany, L. C., B. H. Wilkinson, and D. S. Jones (2003), Using stable isotope data to resolve rate and duration of growth throughout ontogeny: An example from the surf clam, *Spisula Solidissima Palaios*, *18*(2), 126–137.

Johnson, M. A., and I. V. Polyakov (2001), The Laptev Sea as a source for recent Arctic Ocean salinity changes, *Geophys. Res. Lett.*, *28*(10), 2017–2020.

Jones, D. S. (1981), Repeating layers in the molluscan shell are not always periodic, *J. Paleontol.*, *55*(5), 1076–1082.

Karcher, M. J., R. Gerdes, F. Kauker, and C. Köberle (2003), Arctic warming: Evolution and spreading of the 1990s warm event in the Nordic seas and the Arctic Ocean, *J. Geophys. Res.*, *108*(C2), 3034, doi:10.1029/2001JC001265.

Khim, B.-K., D. E. Krantz, and J. Brigham-Grette (2001), Stable isotope profiles of last interglacial (Pelukian Transgression) mollusks and paleoclimate implications in the Bering Strait region, *Quat. Sci. Rev.*, *20*, 463–483.

Khim, B.-K., D. E. Krantz, L. W. Cooper, and J. M. Grebmeier (2003), Seasonal discharge of estuarine freshwater to the western Chukchi Sea shelf identified in stable isotope profiles of mollusk shells, *J. Geophys. Res.*, *108*(C9), 3300, doi:10.1029/2003JC001816.

Klein, R. T., K. C. Lohman, and C. W. Thayer (1996), Sr/Ca and $^{13}C/^{12}C$ ratios in skeletal calcite of *Mytilus trossulus*: Covariation with metabolic rate, salinity, and carbon isotopic composition of seawater, *Geochim. Cosmochim. Acta*, *60*, 4207–4221.

Kodina, L. A., and M. P. Bogacheva (2002), POC isotope composition in the Ob estuary as compared with the Yenisei system, *Ber. Polar. Meeresforsch. Rep. Polar Mar. Res.*, *419*, 151–157.

Kodina, L. A., M. P. Bogacheva, L. N. Vlasova, S. L. Meschanov, and S. V. Ljutsarev (1999), Isotope geochemistry of particulate organic carbon in the Yenisei estuary: Sources and regularities of distribution, *Ber. Pol. For. Rep. Polar Res.*, *300*, 91–101.

Kowalik, Z., and A. Y. Proshutinsky (1993), Diurnal tides in the Arctic Ocean, *J. Geophys. Res.*, *98*(C9), 16,449–16,468.

Lutz, R. A., and D. C. Rhoads (1980), Growth patterns within the molluscan shell: An overview, in *Skeletal Growth of Aquatic Organisms*, edited by D. C. Rhoads and R. A. Lutz, pp. 203–254, Springer, New York.

Macdonald, R. W. (2000), Arctic estuaries and ice: A positive-negative estuarine couple, in *The Freshwater Budget of the Arctic Ocean*, edited by E. L. Lewis, pp. 383–407, Springer, New York.

Maykut, G. A. (1986), The surface heat and mass balance, in *Geophysics of Sea Ice*, edited by N. Untersteiner, Springer, New York.

McConnaughey, T. (1989), ^{13}C and ^{18}O isotopic disequilibrium in biological carbonates: I. Patterns, *Geochim. Cosmochim. Acta*, *53*, 151–162.

McConnaughey, T. A., J. Burdett, J. F. Whelan, and C. K. Paull (1997), Carbon isotopes in biological carbonates: Respiration and photosynthesis, *Geochim. Cosmochim. Acta*, *61*, 611–622.

Michener, R., and S. Schell (1994), Stable isotope ratios as tracers in marine aquatic food webs, in *Stable Isotopes in Ecology and Environmental Science*, edited by K. Lajtha and R. Michener, pp. 138–157, Blackwell Sci., Malden, Mass.

Millero, F. J. (1993), What is PSU?, *Oceanography*, *6*(3), 67.

Mueller-Lupp, T., H. Erlenkeuser, and H. A. Bauch (2003), Seasonal and interannual variability of Siberian river discharge in the Laptev Sea inferred from stable isotopes in modern bivalves, *Boreas*, *32*(2), 292–303.

Otterå, O. H., H. Drange, M. Bentsen, N. G. Kvamstø, and D. Jiang (2003), The sensitivity of the present-day Atlantic meridional overturning circulation to freshwater forcing, *Geophys. Res. Lett.*, *30*(17), 1898, doi:10.1029/2003GL017578.

Owen, R., H. Kennedy, and C. Richardson (2002), Isotopic partitioning between scallop shell calcite and seawater: Effect of shell growth rate, *Geochim. Cosmochim. Acta*, *66*, 1727–1737.

Parkinson, C. L., and W. M. Washington (1979), A large scale numerical model of sea ice, *J. Geophys. Res.*, *84*(C1), 311–337.

Pavlov, V. K., and S. L. Pfirman (1995), Hydrographic structure and variability of the Kara Sea: Implications for pollutant distribution, *Deep Sea Res., Part II*, *42*(6), 1369–1390.

Peterson, B. J., R. M. Holmes, J. W. McClelland, C. J. Vörösmarty, R. B. Lammers, A. I. Shiklomanov, I. A. Shiklomanov, and S. Rahmstorf (2002), Increasing river discharge to the Arctic Ocean, *Science*, *298*, 2171–2173.

Pivovarov, S., R. Schlitzer, and A. Novikhin (2003), River run-off influence on the water mass formation in the Kara Sea, in *Siberian River Run-off in the Kara Sea: Characterisation, Quantification, Variability, and Environmental Significance*, *Proc. Mar. Sci.*, vol. 6, edited by R. Stein et al., pp. 9–25, Elsevier, New York.

Rahimpour-Bonab, H., Y. Bone, and R. Moussavi-Harami (1997), Stable isotope aspects of modern molluscs, brachiopods, and marine cements from cool-water carbonates, Lacepede Shelf, South Australia, *Geochim. Cosmochim. Acta*, *61*, 207–218.

Renssen, H., H. Goosse, T. Fichefet, and J.-M. Campin (2001), The 8.2 kyr BP event simulated by a global atmosphere-sea-ice-ocean model, *Geophys. Res. Lett.*, *28*(8), 1567–1570.

Rye, D. M., and M. A. Sommer (1980), Reconstructing paleotemperature and paleosalinity regimes with oxygen isotopes, in *Skeletal Growth of Aquatic Organisms*, edited by D. C. Rhoads and R. A. Lutz, pp. 169–202, Springer, New York.

Saenko, O. A., E. C. Wiebe, and A. J. Weaver (2003), North Atlantic response to the above-normal export of sea ice from the Arctic, *J. Geophys. Res.*, *108*(C7), 3224, doi:10.1029/2001JC001166.

Schauer, U., H. Loeng, B. Rudels, V. K. Ozhigin, and W. Dieck (2002), Atlantic water flow through the Barents and Kara seas, *Deep Sea Res., Part I*, *49*(12), 2281–2298.

Schöne, B. R., W. Oschmann, J. Rössler, A. D. Freyre Castro, S. D. Houk, K. Ingrid, D. Wolfgang, J. Ronald, H. Rumohr, and E. Dunca (2003), North Atlantic oscillation dynamics recorded in shells of a long-lived bivalve mollusk, *Geology*, *31*(12), 1037–1040.

Schöne, B. R., A. D. Freyre Castro, J. Fiebig, S. D. Houk, W. Oschmann, and I. Kröncke (2004), Sea surface water temperatures over the period 1884–1983 reconstructed from oxygen isotope ratios of a bivalve mollusk shell (*Arctica islandica*, southern North Sea), *Palaeogeogr. Palaeoclimatol. Palaeoecol.*, *212*, 215–232.

Simstich, J., V. Stanovoy, A. Novikhin, H. Erlenkeuser, and R. F. Spielhagen (2003), Stable isotope ratios in bivalve shells: Suitable recorders for salinity and nutrient variability in the Kara Sea?, in *Siberian River Run-off in the Kara Sea: Characterisation, Quantification, Variability, and Environmental Significance*, *Proc. Mar. Sci.*, vol. 6, edited by R. Stein et al., pp. 111–124, Elsevier, New York.

Simstich, J., V. Stanovoy, D. Bauch, H. Erlenkeuser, and R. F. Spielhagen (2004), Holocene variability of bottom water hydrography on the Kara Sea shelf (Siberia) depicted in multiple single-valve analyses of stable isotopes in ostracods, *Mar. Geol.*, *206*(1–4), 147–164.

Steele, M., and W. Ermold (2004), Salinity trends on the Siberian shelves, *Geophys. Res. Lett.*, *31*, L24308, doi:10.1029/2004GL021302.

Stein, R., and O. Stepanets (2000), Scientific cruise report of the Joint Russian-German Kara-Sea Expedition of RV "*Akademik Boris Petrov*" in 1999, *in Ber. Pol. For. Rep. Polar Res.*, *360*, 1–141.

Stein, R., and O. Stepanets (2001), The German-Russian Project on Siberian River Run-off (SIRRO): Scientific cruise report of the Kara-Sea Expedition "SIRRO 2000" of RV "*Akademik Boris Petrov*" and first results, in *Ber. Polar Meeresforsch. Rep. Polar Mar. Res.*, *393*, 1–287.

Tallqvist, M. E., and J. H. Sundet (2000), Annual growth of the cockle *Clinocardium ciliatum* in the Norwegian Arctic (Svalbard area), *Hydrobiologia*, *440*, 331–338.

Tanaka, N., M. C. Monaghan, and D. M. Rye (1986), Contribution of metabolic carbon to mollusc and barnacle shell carbonate, *Nature*, *320*, 520–523.

Tarutani, T., R. N. Clayton, and T. K. Mayeda (1969), The effect of polymorphism and magnesium substitution on oxygen isotope fractionation between calcium carbonate and water, *Geochim. Cosmochim. Acta*, *33*, 987–996.

Thompson, D. W. J., and J. M. Wallace (2000), Annular modes in the extratropical circulation: Part I. Month-to-month variability, *J. Clim.*, *13*(5), 1000–1016.

Volkov, V. A., O. M. Johannessen, V. E. Borodachev, G. N. Voinov, L. H. Pettersson, L. P. Bobylev, and A. V. Kouraev (2002), *Polar Seas Oceanography—An Integrated Case Study of the Kara Sea*, 450 pp., Springer, New York.

Wegner, C., J. A. Hölemann, I. Dmitrenko, S. Kirillov, K. Tuschling, E. Abramova, and H. Kassens (2003), Suspended particulate matter on the Laptev Sea shelf (Siberian Arctic) during ice-free conditions, *Estuarine Coastal Shelf Sci.*, *57*, 55–64.

Weidman, C. R., G. A. Jones, and K. C. Lohmann (1994), The long-lived mollusc *Arctica islandica*: A new paleoceanographic tool for the reconstruction of bottom temperatures for the continental shelves of the northern North Atlantic Ocean, *J. Geophys. Res.*, *99*(C9), 18,305–18,314.

Wilkinson, B. H., and L. C. Ivany (2002), Paleoclimatic inference from stable isotope profiles of accretionary biogenic hardparts: A quantitative approach to the evaluation of incomplete data, *Palaeogeogr. Palaeoclimatol. Palaeoecol.*, *185*, 95–114.

Winsor, P., and D. C. Chapman (2002), Distribution and interannual variability of dense water production from coastal polynyas on the Chukchi Shelf, *J. Geophys. Res.*, *107*(C7), 3079, doi:10.1029/2001JC000984.

Wotton, R. S. (1990), The classification of particulate and dissolved matter, in *The Biology of Particles in Aquatic Systems*, edited by R. S. Wotton, pp. 1–8, CRC, Roca Baton, Fla.

Zhou, G.-T., and Y.-F. Zheng (2003), An experimental study of oxygen isotope fractionation between inorganically precipitated aragonite and water at low temperatures, *Geochim. Cosmochim. Acta*, *67*, 387–399.

D. Bauch, Leibniz Institute for Marine Sciences (IFM-GEOMAR), Wischhofstrasse 1-3, D-24148 Kiel, Germany. (dbauch@ifm-geomar.de)

H. Erlenkeuser, Leibniz-Laboratory for Radiometric Dating and Stable Isotope Research, Kiel University, Max-Eyth-Strasse 11, D-24118 Kiel, Germany. (herlenkeuser@leibniz.uni-kiel.de)

I. Harms, Institute for Oceanography, University of Hamburg, Bundesstrasse 53, D-22146 Hamburg, Germany. (harms@ifm.uni-hamburg.de)

M. J. Karcher, Alfred-Wegener-Institute for Polar and Marine Research, Columbusstrasse, D-27568 Bremerhaven, Germany. (mkarcher@awi-bremerhaven.de)

L. Kodina, Vernadsky Institute of Geochemistry and Analytical Chemistry, RAS, 19 Kosygin ul., 117975 Moscow, Russia. (kodina@geokhi.ru)

J. Simstich, Department of Earth Sciences, University of Cambridge, Downing Street, Cambridge CB2 3EQ, UK. (jsim03@esc.cam.ac.uk)

R. F. Spielhagen, Leibniz Institute for Marine Sciences (IFM-GEOMAR), Wischhofstrasse 1-3, D-24148 Kiel, Germany. (rspielhagen@ifm-geomar.de)

V. Stanovoy, Arctic and Antarctic Research Institute, 38 Bering ul., 199397 St. Petersburg, Russia. (stanovoy@lens.spb.ru)